Molecular Directionality in Cellulose Polymorphs

Nam-Hun Kim,[†] Tomoya Imai,[‡] Masahisa Wada,[§] and Junji Sugiyama*[,¶]

College of Forest Sciences, Kangwon National University, Chunchon 200-701, Korea, Graduate School of Science, Kyoto University, Kitashirakawa Oiwakecho, Kyoto 606-8502, Japan, Graduate School of Agricultural and Life Sciences, The University of Tokyo, Yayoi, Tokyo 113-8657, Japan, and Research Institute for Sustainable Humanosphere, Kyoto University, Uji, Kyoto 611-0011, Japan

Received September 4, 2005; Revised Manuscript Received October 27, 2005

The recently developed technique of reductive amination, followed by gold labeling, was applied to visualize the reducing ends of cellulose microcrystals from cellulose I, cellulose II, and cellulose III_I. In these crystals, which were also characterized by electron diffraction, the labeling proved that the chains were organized in a parallel fashion in cellulose I from ramie and *Valonia* and also in cellulose III_I from *Valonia*. In microcrystals of cellulose II from mercerized ramie, the labeling method showed that the chains were packed into an antiparallel mode. These results are discussed in terms of the fine structure of cellulose I where neighboring microfibrils of opposite polarity are visualized. The mercerization process whereby cellulose I is converted into cellulose II is therefore best described in terms of an intermingling of the cellulose chains from neighboring microfibrils of opposite polarity. As opposed to the case of mercerization the conversion of cellulose I into cellulose III_I does not require the participation of neighboring microfibrils since the crystalline domains are converted individually.

Introduction

In the mercerization process, which is more than 150 years old,[1] cotton yarns are continuously dipped into a strong alkali solution and then washed and dried. Following this treatment, the yarns acquire a silklike appearance, and there is a drastic polymorphic modification of the crystalline state of the samples that go from cellulose I to cellulose II. Remarkably, the same crystalline cellulose II is also obtained when cellulose is spun or regenerated from solutions in the viscose or other spinning processes. The analyses of the X-ray and neutron fiber diffraction diagrams of cellulose I and II have led to the conclusion that in cellulose I the chains were packed in a parallel fashion (i.e., with their reducing ends always on the same side within the crystalline domains), whereas in cellulose II, antiparallel arrangement was favored (i.e., with their reducing ends alternatively on either side within the crystalline domains).[2−8] Such result, applied to the mercerization process—which is essentially a solid-state transformation—raises a fundamental question, which is to understand how a yarn containing parallel cellulose chains can become arranged into an antiparallel packing without going into solution. The answer to such question is still raising many debates, where the results from diffraction analyses are sometimes questioned.[9−11] There is therefore a need to find other experimental techniques to identify the polarity of the chains both in cellulose I and II.

The treatment of cotton with liquid ammonia is another process, which influences the properties of cotton fabrics, giving them enhanced dyeability and softness. In this case, the crystalline structure is converted from cellulose I into cellulose III_I, and there is a consensus showing that in cellulose III_I, as in cellulose I, the chains are crystallized in a parallel fashion.[12−14] Thus, unlike in the mercerization process, there is no conceptual ambiguity in interpreting the conversion of cellulose I into cellulose III_I.

Apart from crystallography, the specific staining of the reducing ends of the cellulose chains is another independent approach that should clarify the problem of polarity of the cellulose chains during the transformation of cellulose I into cellulose II. Hieta et al.[15] and later Kuga and Brown[16] and Koyama et al.[17] have devised and used a silver-staining technique designed to identify the reducing ends of cellulose I microcrystals from *Valonia*, ramie, and bacterial cellulose. The technique showed that only one end of some microcrystals were labeled and not the other. The reducing ends silver-staining technique was further modified and improved in our laboratory by adding biotin hydrazide to the cellulose reducing ends followed by an interaction with streptavidin−gold nanoparticles observable by transmission electron microscopy (TEM). This technique appears general for polysaccharide crystals as we could implement it for highly crystalline β-chitin microfibrils and microcrystals,[18,19] which had proven resistant to the silver-labeling method. In combining this technique with electron crystallography experiments, we were able to identify the directionality of cellulose and β-chitin biosynthesis.[20−22]

So far, the reducing ends labeling technique has not been applied to cellulose polymorphs other than cellulose I. In the present paper, we have used it to follow the polarity of the cellulose chains in the solid-state conversion of cellulose I into cellulose III_I and that of cellulose I into cellulose II. The resulting images, together with surface replicas and electron crystallography data, have allowed us to propose a scheme describing the mercerization process at the molecular level.

Materials and Methods

Plant Materials. Ramie: purified native ramie (*Boehmaria nivea* Gaud), a gift from Professor Emeritus Okano, the University of Tokyo, was used as starting material.

Vesicles of *Valonia* (*V. macrophysa and V. ventricosa*), preserved in 10% formaldehyde in seawater, were purified using the following

* Corresponding author. Fax: +81-774-38-3635. E-mail: sugiyama@rish.kyoto-u.ac.jp.

[†] Kangwon National University.

[‡] Graduate School of Science, Kyoto University.

[§] The University of Tokyo.

[¶] Research Institute for Sustainable Humanosphere, Kyoto University.

10.1021/bm0506391 CCC: $33.50
Published on Web 12/08/2005

procedure. The vesicles were boiled in an excess of 1% aqueous NaOH for 6 h with a fresh solution exchange after 2 h and followed by thorough washing in distilled water. The vesicles were then soaked overnight in 0.5 N HCl at room temperature followed by further washing in distilled water. The whole treatment was repeated twice until the vesicles became completely translucent and colorless.

Cellulose III_I Preparation. Purified vesicles of *Valonia ventricosa* were subjected to liquid ammonia treatment under supercritical condition,[13] leading to a complete conversion to cellulose III_I, confirmed by X-ray diffraction. The vesicles were then hydrolyzed by 50% H_2SO_4 at 50 °C for 1 h under constant stirring. The resulted microcrystalline preparation was verified by FTIR spectroscopy and X-ray diffraction to ensure that the treatment did not bring any reversion of cellulose III_I to cellulose I.

Mercerization. Ramie: 100 purified ramie fibers of ca. 10 cm length were carefully aligned to make up a bundle, which was fixed to a Teflon plate. The design of this plate not only ensured that the fibers experienced mercerization under tension but also allowed us to follow the transformation by X-ray diffraction. The fibers were mercerized in a 3.5 N NaOH aqueous solution followed by thorough washing in distilled water and air-drying. The treatment was repeated until the X-ray diffraction diagram of the sample showed complete conversion to cellulose II. The mercerized ramie fibers were then hydrolyzed by boiling in 2.5 N HCl for 1 h. The resulted microcrystalline preparation was checked by electron and X-ray diffraction to ensure that the treatment did not bring any reversion to cellulose I.

Whole vesicles of *V. macrophysa*, having about 1 cm in diameter, were immersed in 8 N NaOH aqueous solution at 25 °C for various times ranging from 1 to 30 min. Extensive shrinkage occurred as the volumes became only 70%, 50%, 30%, and 20% of that of the initial vesicles after treatments of respectively 1, 5, 10, and 30 min. The vesicles were then washed thoroughly in distilled water followed by air-drying.

Surface Replication. Vesicles of *V. macrophysa* mercerized for 1, 5, 10, and 30 min were washed thoroughly with distilled water and were finally freeze-dried. The exterior surface of the vesicles was shadowed by Pt/Pd followed by carbon coating, and the coated side was then reinforced by thermally softened polystyrene mold. After hardening by cooling, the molds were immersed with the polystyrene down in a chromic−sulfuric acid solution that dissolved the cell wall materials and released the replica from the polystyrene mold. The replicas were washed by floating in several freshwater baths and mounted on EM grids.

Ultrathin Sectioning. To visualize the statistical distribution of "up" and "down" microfibrils in one lamella of the *Valonia* cell wall, a fragment of a *V. ventricosa* cell wall was embedded in epoxy resin and ultrathin sections of 70 nm thickness were prepared.

To follow the ultrastructural modification occurring during mercerization, mercerized (30 min treatment) and control cell walls of *V. macrophysa* were embedded in epoxy resin (Epon 812 hard mixture, Oken, Japan) and ultrathin sections of about 90 nm thick were cut by an ultramicrotome equipped with a diamond knife. The sample was carefully oriented to ensure that the one of two major microfibrillar cellulose orientations in the cell wall was perpendicular to the cutting direction. This allowed us to visualize the microfibril cross section by diffraction contrast TEM.

Labeling of the Reducing Ends. The previously reported technique using biotin and streptavidin[18] was used for the TEM visualization of the reducing ends of microfibrils. First, purified samples were boiled in 2.5 N HCl to have well-dispersed microcrystalline specimens, desirable for judging easily if the labels were on a single or composite microcrystals. All the samples were used directly for the labeling experiments, with the exception of *Valonia* microcrystals, which were subjected to a cellulase digestion prior to the labeling protocol. Here, we used a purified Cel6A (former CBHII)—a kind gift from Dr. A. Koivula, VTT Biotechnology, Finland—an enzyme produced by a *Trichoderma reesei* strain devoid of Cel7B (former EG1) and Cel5A (former EG2) genes. Cel6A is known to attack exclusively the nonreducing ends of cellulose chains,[23] inducing a marked tapering at the corresponding ends of the cellulose microcrystals.[24] An amount of 0.5 mL of 0.5 mg/mL *Valonia* microcrystals in water was mixed with 1 mL of 2.8 mg/mL enzyme in 20 mM acetate buffer at pH 4.5. The mixture was incubated at 27 °C for 12 h, and the digestion was terminated by washing in 0.2% aqueous NaOH, followed by thorough washing in distilled water. The various microcrystals were suspended in 1 mL of absolute methanol and 50 μL of acetic acid. Biotinylation was initiated by adding 3 mg of biotinamidocaproyl hydrazide (BXH) and 0.3 mg of $NaBH_3CN$ to this suspension and heating it at 50 °C for 12−16 h in the presence of molecular sieves 3A. The suspension was centrifuged for exchanging the solvent against blocking buffer (10 mM phosphate buffer (pH 7.0), 150 mM NaCl, 0.02% Tween 20, and 0.5% bovine serum albumin). After incubating for 30 min at 37 °C for blocking, the suspension of biotinylated microfibrils was incubated with 100-fold dilution of streptavidin−gold (Φ = 10 nm, Sigma Co., U.S.A.) for 1 h at 37 °C. The labeled microfibrils were washed twice with 50 mM phosphate buffer (pH 7.0) including 0.02% Tween 20 and then twice with distilled water by successive centrifugations. All the reactions were carried out in glass vials prewashed by nitric acid. For control, a labeling experiment was achieved following a chain end reducing treatment resulting from an interaction with 2% $NaBH_4$ at 40 °C for 72 h. This treatment converted the hemiacetal groups located at the reducing end of the cellulose chains into secondary alcohol, which was not stained in our protocol.

Low-Dose Electron Microscopy. The micrographs and diffraction diagrams were taken with a JEOL-2000EX II TEM operated at 100 kV and recorded on Mitsubishi MEM film. Diffraction contrast imaging in the bright and dark field mode was used to visualize the sample without further contrast enhancement. The images were taken at 2500−6000× under low-dose exposure with the use of a minimum dose system (MDS, JEOL, Japan).

The electron diffraction diagrams were obtained in the microdiffraction mode. For this, a small condenser aperture of 20 μm was inserted in the second condenser lens and the first condenser lens was fully overfocused to achieve an electron probe of approximately 100 nm at the sample level. The samples were observed at 2500× under extremely low-dose conditions, at the limit of the dark current, with the help of an image intensifier (fiber optics coupled TV, Gatan). After proper zone identification, the beam was manually blanked. The beam intensity was then set to the desired value, and the electron microscope was switched to the diffraction mode. The beam was deblanked, followed immediately by the opening of the mechanical shutter and the recording of the diffraction diagram on a preset film. This procedure allowed diffraction diagrams to be taken not only on individual *Valonia* microcrystals but also on microcrystals of ramie and cellulose II samples.

Results

***Valonia* Cellulose I and III_I.** Parts a−d of Figure 1 are typical examples of *Valonia* cellulose I microcrystals after digestion with Cel6A followed by labeling. During this enzymatic treatment, the nonreducing ends of the microcrystals are specifically hydrolyzed,[23] leaving tapered tips, whereas the reducing ends remained blunt.[24] Our biotin/streptavidin−gold technique was quite efficient to label the reducing ends of these samples. Following the labeling operation, most microcrystals displayed a gold particle at their blunt reducing ends but never at the nonreducing tapered ends. In the inset, a typical spot electron diffraction diagram, recorded on one individual microcrystal, clearly indicates that this element is an individual whiskerlike single crystal of the cellulose Iα type, a crystalline allomorph containing only one chain per unit cell.[8,25] Thus, by combining the information from digestion, labeling, and diffraction, it is clear than in a given microcrystal of *Valonia*, all

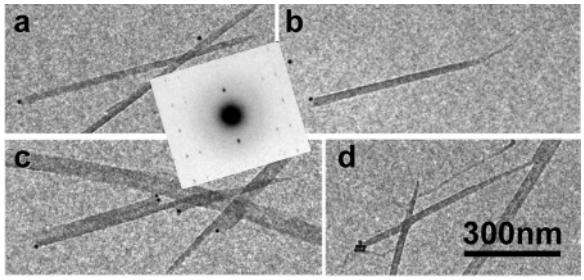

Figure 1. Reducing ends labeling of *V. ventricosa* cellulose I microcrystals predigested by Cel6A (a−d). Note the unlabeled tapered ends corresponding to the nonreducing ends, while the other blunt ends, with their reducing end labeling, keep the initial shape of the microcrystals before the enzymatic treatment. Multiple labeling occurs occasionally as in (d). Inset: typical electron diffraction pattern recorded on one microcrystal indicative of a single-crystal diagram indexed as cellulose Iα.

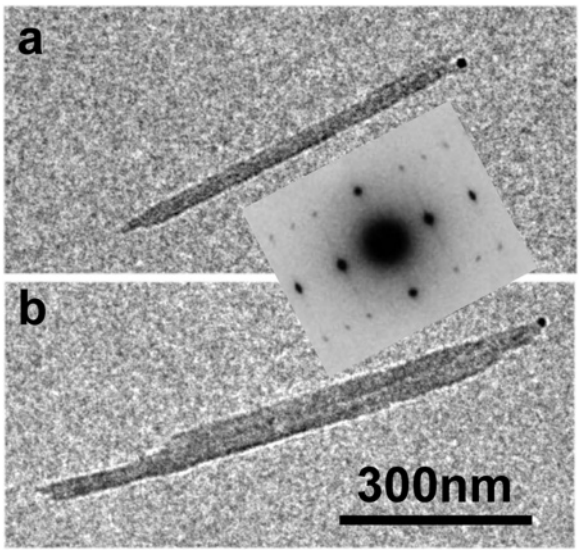

Figure 2. Reducing ends labeling of *V. ventricosa* cellulose III_I microcrystals (a and b). The initial microcrystalline nature of cellulose I has been maintained. The complete transformation into cellulose III_I was verified by FTIR spectroscopy and X-ray diffraction analysis. Inset: typical electron diffraction pattern recorded on one microcrystal indicating that the conversion proceeded in an intrafibrillar manner.

the cellulose chains are crystallized in a parallel fashion, with all their reducing ends on the same side.

Parts a and b of Figure 2 correspond to microcrystals of *Valonia* that have been converted into cellulose III_I. During this treatment, the monocrystalline character of the microcrystal is maintained, as each microcrystal yields a spot electron diffraction pattern of cellulose III_I (inset). In addition, the gold labeling is clearly evidenced at one of the tips of these elements, confirming also the parallel organization of the cellulose chains in the crystal of cellulose III_I.

Conversion of *Valonia* I into *Valonia* II. When the total mercerization of a *Valonia* sample was achieved by immersion in 8 N NaOH for 30 min, the *Valonia* vesicles became rather transparent and their volume was drastically reduced to only about 20% of the initial volume. In addition to this shrinkage, the transformation induced a modification of the cell wall morphology, which was progressive with time. This is illustrated in parts a−d of Figure 3, which correspond to a series of surface replicas of a vesicle, taken as a function of alkali immersion time. Initially, the surface of the cell wall displays a series of superimposed crisscrossed layers, each containing a parallel array of endless microfibrils with sharp contours (Figure 3a).

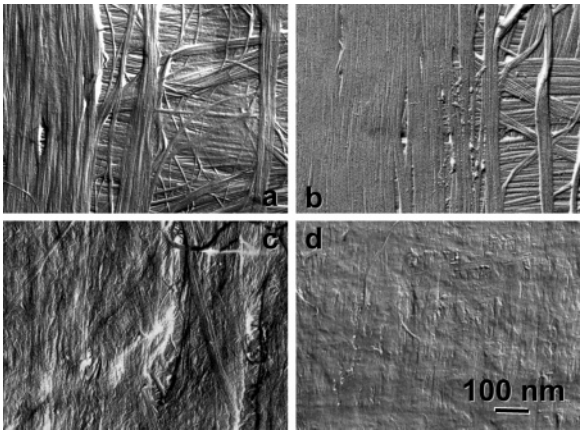

Figure 3. Images of surface replicas of a *V. macrophysa* cell wall during the mercerization process in 8 N aqueous NaOH. The alkaline treatment was 1 min (a), 5 min (b), 10 min (c), and 30 min (d), respectively. With mercerization time, the contours of the microfibrils became dull followed by the merging into large bundles (a−c). At the final stage, the microfibrillar nature of the initial cellulose I could not be seen any more (d).

After 5 min, the individual initial microfibrils have merged into broader ribbons, but the microfibrillar layers can still be observed (Figure 3b). After 10 min, the initial microfibrillar morphology and the cell wall layering are lost, but still the microfibril direction can be detected (Figure 3c). After 30 min (Figure 3d), all microfibrillar information is erased and only the directionality of the surface layer is still barely discernible.

The examination of cross sections of *Valonia* cell wall fragments before and after mercerization gives further insight on the inner morphology of the wall and its modification during the treatment. Before mercerization, a diffraction contrast image in bright field mode (Figure 4a) reveals the crystalline nature of the microfibrils, in the areas where they are cut perpendicular to their long direction. This image reveals the section of each microfibril as a squarish black dot with a side of about 20 nm. The corresponding electron diffraction diagram (inset in Figure 4a) indicates that in such layer, the crystalline microfibrils are uniplanar, with their 0.6 nm planes, indexed as (100), in the triclinic system,[25] parallel to the wall surface. Another key feature of this diagram is that the 110 diffraction spots (d = 0.39 nm) are split along two diagonal directions (arrows). This splitting and its analysis, schematically explained in Figure 4, parts c and d, confirm that in a microfibrillar layer of *Valonia* cellulose, there exists two opposite directionalities of the cellulose chain axis *c* and therefore two types of microfibrils, some going upward perpendicular to the plane of Figure 4a and others going downward.[26−28] This duality is further demonstrated by dark field images (Figure 5, parts a and b) using the diffraction spots belonging to one or the other pairs of the 110 traces (Figure 5d) to create each image. The technique, which reveals the microfibrils section as white squarish dots, allows us to identify the microfibrils running upward or downward. By combining two dark field images from the two directions, it becomes apparent that there is a statistical distribution of the microfibril polarity within each layer of the *Valonia* cell wall (Figure 5c). In cross section, a mercerized sample *Valonia* cell wall (Figure 4b) presents a morphology that is totally different from that of the initial sample. Indeed, a diffraction contrast image reveals a number of very small crystalline domains, with no definite shape or regularity. As opposed to the high textural order in the initial *Valonia* cell walls, there is a total loss of orientation of the crystalline domains with respect to the cell

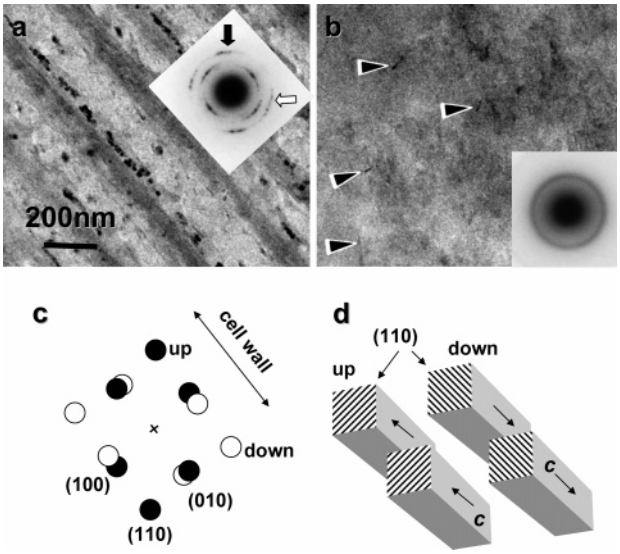

Figure 4. Cross-sectional view of a *V. macrophysa* cell wall before and after mercerization. In (a), the initial squarish microfibrils in cross section are seen as dark dots, organized in layers. Inset: typical oriented electron diffraction diagram of cellulose Iα, recorded on one layer of perpendicular microfibrils. The black arrow points toward the 110 diffraction spot corresponding to microfibrils that go upward with respect to the section plane, whereas the white arrow corresponds to microfibrils running downward, as explained in (c) and (d). (b) As in (a), but after mercerization (15 min treatment). The sections of the crystalline domains appear as black somewhat elongated dots (arrowheads) randomly dispersed in the section. Inset: typical unoriented electron diffraction diagram indicating that the sample is fully converted into cellulose II. (c) Schematic electron diffraction diagram of (a). (d) Corresponding schematic set of cellulose microfibrils of opposite polarities.

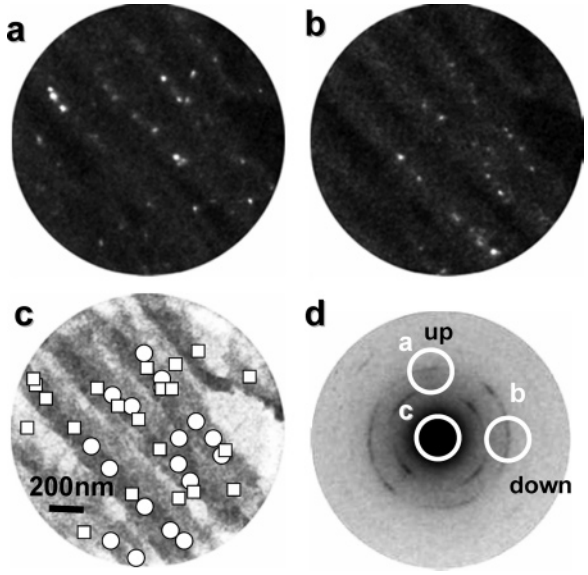

Figure 5. Typical dark field images of a cross section of *V. ventricosa* as in Figure 4a. In Figure 5, (a) was recorded with the use of the 110 spot corresponding to microfibrils running upward (see part d for explanation) and (b) was obtained with the 110 spot corresponding to microfibrils running downward. (c) Corresponding bright field image recorded with only the central electron beam (see part d for explanation). In this image, the squares correspond to microfibrils running upward, whereas the circles are those running downward. (d) A diffraction pattern taken from the corresponding area. White circles indicate the position of objective aperture for obtaining images in (a)−(c) respectively.

wall surface in the *Valonia* II samples. The electron diffraction diagram (inset in Figure 4b) shows that the diffraction traces

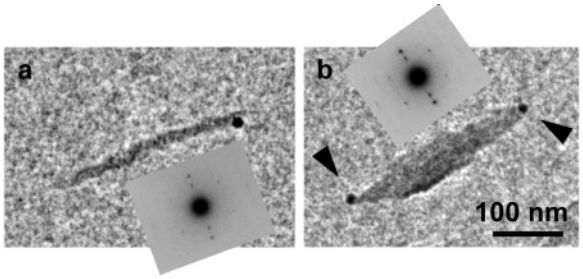

Figure 6. (a) Ramie cellulose I microcrystal labeled at one end demonstrating that the chains in ramie microfibrils are packed in a parallel mode. Inset: typical electron diffraction taken of a similar microcrystal. (b) A bundle of ramie microcrystals tightly associated. Exceptionally, a labeling is observed at both ends (arrowheads) but misaligned with respect to the microcrystal direction. Inset: typical electron diffraction diagram taken on such bundle.

of cellulose have become perfectly circular. This diagram, which differs significantly from the oriented pattern of *Valonia* I (inset in Figure 4a), confirms the randomization of the crystalline domains during mercerization.

Ramie Cellulose I. Bast fibers from ramie have been frequently used for the structural studies of cellulose, due to the nearly perfect alignment of the microfibrils along the axis of these fibers. In ramie, the lateral size of the microfibrils are nearly $^1/_5$ of those of *Valonia*. Nevertheless, lattice imaging has shown that the crystalline domains of ramie were as perfect as those of *Valonia*.[29] Our labeling technique proved to be efficient to label only one end of the ramie microcrystals (Figure 6a), thus confirming the parallel organization of the cellulose chains in these elements. Unlike the case of *Valonia,* where each microcrystal gave a unique spot diffraction diagram, even the smallest ramie microcrystal appears to be composed of a tight packet of two or three crystalline domains with different orientations about the microcrystal axis. Indeed, the diffraction patterns of most microcrystals (inset in Figure 6a) present two or more sets of equatorial diffraction pairs, $\bar{1}10$, 110 and/or 200 (indexed along the cellulose Iβ monoclinic unit cell[25]). Despite this multiplicity, the unique labeling indicates that in the corresponding microcrystal, all the crystalline domains have the same polarity.

In the case of larger elements, consisting of a bundle of five to six individual crystals (Figure 6b), a labeling at both ends (see arrows) of the microcrystal is exceptionally observed. In that case, however, the two labels are not aligned along the microcrystal axis but occur in a diagonal arrangement. As in the case of the inset in Figure 6a, the electron diffraction pattern inset in Figure 6b indicates that there are a number of crystals in this element. Nevertheless, the number of small and independent crystalline domains in Figure 6b is larger than those in Figure 6a since the diffraction pattern inset in Figure 6b is a real fiber diagram of cellulose I, indicative of a number of coaxial crystalline domains organized along a cylindrical symmetry. The two-ends labeling in diagonal with respect to the microcrystal axis is thus an indication that, in ramie as in *Valonia* cellulose, there are adjacent crystalline domains with opposite polarity that are close to one another.

Ramie Cellulose II. In the microcrystalline samples prepared from mercerized ramie, the microcrystals of cellulose II were still elongated but much shorter (Figure 7a−e) than those of cellulose I from ramie. Their lateral size is variable, as the narrowest are no more than 2 nm, whereas the larger ones are 10 times wider. In addition, whereas the smallest microcrystals are fairly linear, the broadest ones have less regular shapes.

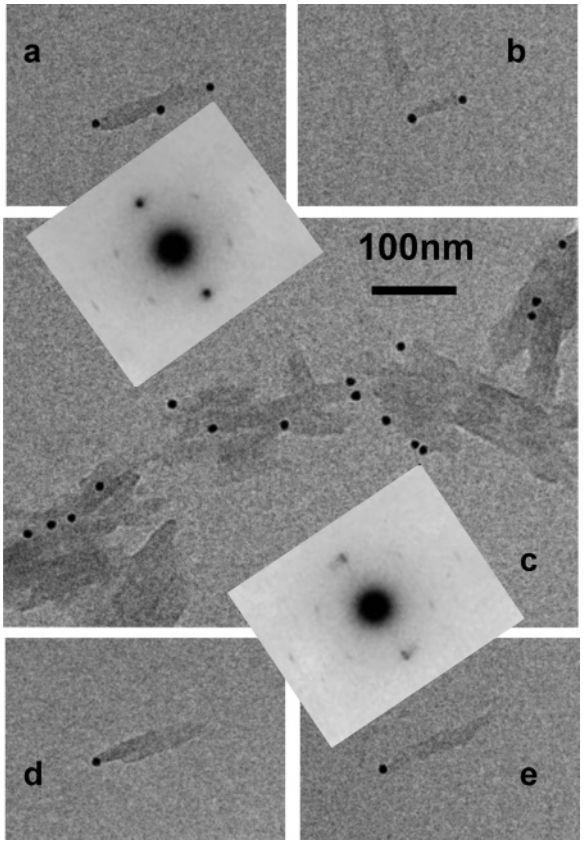

Figure 7. Labeled microcrystals of mercerized ramie. Labels are clearly seen on both ends of the microcrystals (a and b) and only one end (d and e). In most cases however (c), the microcrystals are aggregated into clusters, where individual particles are difficult to identify. By electron diffraction (insets) the molecular orientation, i.e., the *c*-axis of cellulose II, can be identified, and it is always parallel to the long direction of the microcrystals. Quite interestingly, the upper inset diagram, which corresponds to a single-crystal diagram, was taken from a platelike microcrystal broader than the initial ramie I microcrystals.

When probed by electron diffraction (insets), each crystal yields a well-oriented cellulose II pattern, indicating that in these, the cellulose chains are aligned along the axis of these microcrystals. As in the diffraction patterns of ramie I, most patterns of ramie II present more than one spot on their equatorial layer lines (lower inset in Figure 7). Thus, in the corresponding microcrystals, there are several crystalline domains, rotated with respect to one another about the microcrystal axes. Occasionally, the diffraction diagram from one of the largest microcrystals gave a strong diffraction diagram, containing only one pair of equatorial spots (upper inset in Figure 7). This microcrystal, which is wider than those of the initial ramie, consists therefore of only one rather large crystalline domain, created during the mercerization process, when the alkali is washed away.

In surveying the microcrystals in Figure 7, most of them present some labeling. A small percentage of about 15% were labeled at both ends (Figure 7, parts a and b) and quite a few more at only one end (Figure 7, parts d and e). A number microcrystals (Figure 7c) display multiple labeling at their ends or sometimes in their middle, indicating the composite nature of these elements.

Discussion

Among the results that are presented here, those related to the polymorphic transformations of *Valonia* cellulose are the most straightforward. Our diffraction data confirm that the microcrystals of native *Valonia* have indeed a monocrystalline character. Following the most recent crystallography analysis of cellulose Iα and Iβ,[7,8] these crystals consist therefore of an assembly of parallel chains with all their reducing ends on the same side. This organization is confirmed independently from crystallography by the digestion of the microcrystals by Cel6A, acting selectively at the nonreducing ends[23] and our labeling protocol, which attaches gold particles and the reducing ends (Figure 1).

The present observations on the solid-state transformation *Valonia* I → *Valonia* III_I can be evaluated in terms of earlier reports. In fact, the ultrastructural features of the transformation of cell wall fragments of *Valonia* I into *Valonia* III_I has been already investigated, using anhydrous ethylenediamine (EDA) as the intracrystalline swelling agent, followed by washing in ethanol.[30−32] In these earlier studies, it was shown that not only the microfibrillar integrity of the wall was maintained during the transformation but also that each microfibril of cellulose I was converted into a microfibril of cellulose III_I without intermingling with its neighbors. Nevertheless, the conversion through the EDA route induced a substantial number of defects within the microfibrils of cellulose III_I.[30−32] These defects could be well visualized by diffraction contrast electron microscopy. In the present paper, we have used the route of supercritical liquid ammonia, which is far superior to improve the resulting crystallinity of cellulose III_I.[13] Under our experimental conditions, the microcrystals of this allomorph do not show the defects reported earlier but rather occur as monocrystalline objects. In addition, there is a perfect agreement between the parallel chain arrangement in the crystals of cellulose III_I[14] and the exclusive labeling of these crystals at only one of their ends. Given these observations and the recent crystallographic analyses of cellulose I and III_I,[7,8,14] the understanding of the mechanism of the solid-state transformation of *Valonia* I → *Valonia* III_I does not present any major difficulty since the parallel chain crystals of cellulose I become converted into parallel chain crystals of cellulose III_I. There are minor modifications in the crystal structure when going from cellulose I to cellulose III_I, namely, the translation of half of the cellulose chains with respect to one another by a quarter of a unit cell and the rotation of the hydroxymethyl group, which goes from the *tg* conformation in cellulose I to *gt* in cellulose III_I.[33] These modifications must have had some influence on the crystalline perfection of cellulose III_I when the EDA route was used. In the present case, the monocrystalline character of the *Valonia* III_I microcrystals is a clear indication that the cellulose I → cellulose III_I transformation, which uses ammonia at high temperature and pressure, is beneficial to create superior cellulose III_I crystals.

The solid-state transformation *Valonia* I → *Valonia* II under the influence of strong aqueous NaOH is more profound as the concomitant extensive swelling destroys the initial microfibrillar morphology of the cell wall, allowing the cellulose chains to reach a substantial mobility within the wall (Figure 3a−d). In cross section (Figure 4b) one sees that the resulting cellulose II crystals have no common features with those of the initial cell wall. This observation, already reported by Bradford and Revol,[34] confirms the reshuffling occurring during the recrystallization in the form of cellulose II. Within a layer of cellulose microfibrils in native *Valonia*, it had been known for a number of years that there were two families of microfibrils of opposite polarity.[26−28] Our dark field images in Figure 5, parts a and b, confirm this occurrence, and for the first time, we are even able to tag the microfibrils of each polarity within a given cell wall

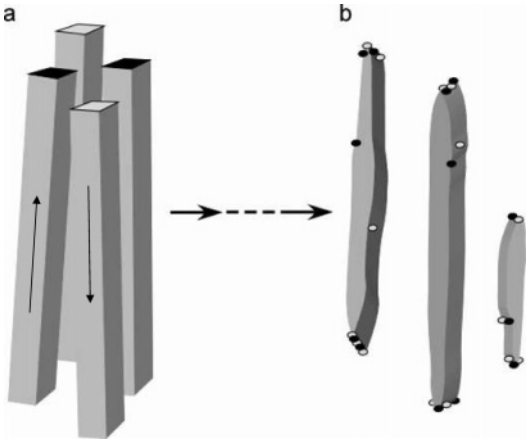

Figure 8. Schematic conversion of microcrystals of ramie I (a) into ramie II (b). In (b) the dark dots correspond to chain ends of "up" polarity whereas the white dots correspond to chain end of "down" polarity.

layer. These images indicate that there is a statistical distribution of "up" and "down" microfibrils with respect to the sectioning plane and that there are roughly the same number of microfibrils running in each direction, the "up" microfibrils being never too far from the "down" microfibrils. Thus, during the mercerization process, the "up" and "down" cellulose chains, which are liberated from the microfibrillar constraints, are free to coalesce and interdigitate to yield the antiparallel crystals of cellulose II that are renown to be more thermodynamically stable than those of cellulose I. The mechanism of interdigitation was already proposed as a possibility by Okano and Sarko[35] to cope with the difficulty of explaining the polarity reversal of half of the cellulose chains during mercerization. In the present paper we bring further support to this hypothesis by demonstrating that indeed, at least in the *Valonia* cell wall, there are antiparallel microfibrils in close contact, ready to merge into one another if sufficient swelling is applied.

In the case of native ramie, the limit of the current electron microscopy technique does not allow us to clearly identify each crystalline domain by its electron diffraction spectrum. The electron diffraction diagram in Figure 6, which is taken from one microcrystal, indicates that in this element, there is more than one crystalline domain. With the help of our labeling technique, the polarities of the crystalline domains within a ramie microcrystal are revealed. While in most cases, the cellulose chains in these elements have the same polarity, aggregates of opposite polarity with labeling at both ends are also observed (Figure 6b). This bipolarity is a strong indication that, in ramie fibers as in *Valonia*, the cell walls also consist of an assembly of microfibrils of both polarities: "up" microfibrils being adjacent to "down" microfibrils as schematically shown in Figure 8a. Thus, for ramie as well as for *Valonia*, these microfibrils are ready to intermingle to yield the cellulose II crystals shown in Figure 7 and schematically drawn in Figure 8b. Whereas in cellulose III_I the microcrystals had the same appearance and dimension as the parent microcrystals of cellulose I, this is not so for the cellulose II microcrystals (Figure 7) which have shapes and sizes different from those of the initial ramie I. The fact that some microcrystals are substantially wider is a clear indication that they result from the intermingling of the content of more than one initial cellulose microfibril. In Figure 7, parts a and b, the occurrence of microcrystals labeled at both ends gives a clear indication of antiparallelism in cellulose II. Our observations contradict those of Maurer and Fengel,[36] who used the silver-labeling method to identify the reducing end groups of microcrystals from mercerized cotton. Since, they could not observe microcrystal labeled at both ends, they concluded on a parallel organization of the cellulose chains in cellulose II crystals. To account for the difference between their work and the present one, we believe that our labeling technique is more efficient than the silver labeling to tag the reducing ends of polysaccharide crystals. Such efficiency was proven in the labeling of chitin microcrystals, which are refractive to the silver method, but not in our biotin/streptavidin technique.[18] Also, in the micrographs of cellulose microcrystals labeled with both techniques, the percentage of unlabelled crystals is systematically larger in the silver method.

The mechanism of mercerization by interdigitation can take place only within a cell wall where there are adjacent cellulose microfibrils of opposite polarities. If the microfibrils are not packed into compact cell walls, they cannot coalesce with neighbors of opposite polarity. They are therefore condemned to recrystallize on themselves, with the result of extensive crumpling,[37,38] if the conversion is total, or shish-kebabs in the case where only partial mercerization is achieved.[39,40] The observations of these morphologies are consistent with our model of parallel chains for cellulose I and antiparallel for cellulose II.

Acknowledgment. N.H.K. thanks KOSEF funding for a short term to Japan. A part of this study was supported by Grants-in-Aid for Scientific Research (Nos. 14360099, 14656069, 17580142 to J.S.). The authors thank also Dr. H. Chanzy, for valuable suggestions and critical reading of the manuscript.

References and Notes

(1) Mercer, J. Improvements in the Preparation of Cotton and Other Fabrics and Other Fibrous Materials. Br. Patent 13296, 1850.
(2) Sarko, A.; Muggli, R. Packing analysis of carbohydrates and polysaccharides. III. *Valonia* cellulose and cellulose II. *Macromolecules* **1974**, *7*, 486−494.
(3) Gardner, K. H.; Blackwell, J. The structure of native cellulose. *Biopolymers* **1974**, *13*, 1975−2001.
(4) Stipanovic, A. J.; Sarko, A. Packing analysis of carbohydrates and polysaccharides. 6. Molecular and crystal structure of regenerated cellulose II. *Macromolecules* **1976**, *9*, 851−857.
(5) Kolpak, F. J.; Blackwell, J. Determination of the structure of cellulose II. *Macromolecules* **1976**, *9*, 273−278.
(6) Langan, P.; Nishiyama, Y.; Chanzy, H. A revised structure and hydrogen-bonding system in cellulose II. *J. Am. Chem. Soc.* **1999**, *121*, 9940−9946.
(7) Nishiyama, Y.; Langan, P.; Chanzy, H. Crystal structure and hydrogen bonding system in cellulose Iβ from synchrotron X-ray and neutron fiber diffraction. *J. Am. Chem. Soc.* **2002**, *124*, 9074−9082.
(8) Nishiyama, Y.; Sugiyama, J.; Langan, P.; Chanzy, H.; Langan, P. Crystal structure and hydrogen bonding system in cellulose Iα from synchrotron X-ray and neutron fiber diffraction. *J. Am. Chem.* Soc. **2003**, *125*, 14300−14306.
(9) French, A. D. The crystal structure of ramie cellulose. *Carbohydr. Res.* **1978**, *61*, 67−80.
(10) Kroon-Batenburg, L. M. J.; Kroon, J. The crystal and molecular structure of cellulose. *Carbohydr. Eur.* **1995**, *12*, 15−19.
(11) Marhöfer, R. J.; Reiling, S.; Brickmann, J. Computer simulation of crystal structures and elastic properties of cellulose. *Ber. Bunsen-Ges. Phys. Chem.* **1996**, *100*, 1350−1354.
(12) Sarko, A.; Southwick, J.; Hayashi, J. Packing analysis of carbohydrates and polysaccharides. 7. Crystal structure of cellulose III_I and its relationship to other cellulose polymorphs. *Macromolecules* **1976**, *9*, 857−863.
(13) Wada, M.; Heux, L.; Isogai, A.; Nishiyama, Y.; Chanzy, H.; Sugiyama, J. Improved structural data of cellulose III_I prepared in supercritical ammonia. *Macromolecules* **2001**, *34*, 1237−1243.

(14) Wada, M.; Chanzy, H.; Nishiyama, Y.; Langan, P. Cellulose III_I crystal structure and hydrogen bonding by synchrotron X-ray and neutron fiber diffraction. *Macromolecules* **2004**, *37*, 8548−8555.
(15) Hieta, K.; Kuga, S.; Usuda, M. Electron staining of reducing ends evidences a parallel-chain structure in *Valonia* cellulose. *Biopolymers* **1984**, *23*, 1807−1810.
(16) Kuga, S.; Brown, R. M., Jr. Silver labelling of the reducing ends of bacterial cellulose. *Carbohydr. Res.* **1988**, *180*, 345−350.
(17) Koyama, M.; Sugiyama, J.; Itoh, T. Systematic survey on crystalline features of algal cellulose. *Cellulose* **1997**, *4*, 147−160.
(18) Imai, T.; Watanabe, T.; Yui, T.; Sugiyama, J. Directional degradation of β-chitin by chitinase A1 revealed by a novel reducing end labelling technique. *FEBS Lett.* **2002**, *510*, 201−205.
(19) Hult, E.-L.; Katouno, F.; Uchiyama, T.; Watanabe, T.; Sugiyama, J. Molecular directionality in crystalline β-chitin: hydrolysis by chitinases A and B from *Serratia marcescens* 2170. *Biochem. J.* **2005**, *388*, 851−856.
(20) Koyama, M.; Helbert, W.; Imai, T.; Sugiyama, J.; Henrissat, B. Parallel-up structure evidences the molecular directionality during biosynthesis of bacterial cellulose. *Proc. Natl. Acad. Sci. U.S.A.* **1997**, *94*, 9091−9095.
(21) Sugiyama, J.; Boisset, C.; Hashimoto, M.; Watanabe, T. Molecular directionality of β-chitin biosynthesis. *J. Mol. Biol.* **1999**, *286*, 247−255.
(22) Imai, T.; Watanabe, T.; Yui, T.; Sugiyama, J. The directionality of chitin biosynthesis: a revisit. *Biochem. J.* **2003**, *374*, 755−760.
(23) Rouvinen, J.; Bergfors, T.; Teeri, T.; Knowles, J. K. C.; Jones, T. A. Three dimensional structure of cellobiohydrolase II from *Trichoderma reesei*. *Science* **1990**, *249*, 380−386.
(24) Chanzy, H.; Henrissat, B. Unidirectional degradation of *Valonia* cellulose microcrystals subjected to cellulase action. *FEBS Lett.* **1985**, *184*, 285−288.
(25) Sugiyama, J.; Vuong, R.; Chanzy, H. Electron diffraction study on the two crystalline phases occurring in native cellulose from an algal cell wall. *Macromolecules* **1991**, *24*, 4168−4175.
(26) Sugiyama, J.; Harada, H.; Fujiyoshi, Y.; Uyeda, N. Lattice images from ultrathin sections of cellulose microfibrils in the cell wall of *Valonia macrophysa* Kütz. *Planta* **1985**, *166*, 151−168.
(27) Revol, J. F.; Goring, D. A. I. Directionality of the *c* axis of cellulose crystallites in microfibrils of *Valonia ventricosa*. *Polymer* **1983**, *24*, 1547−1550.
(28) Chanzy, H. In *Cellulose Sources and Exploitation. Industrial Utilization, Biotechnology and Physicochemical Properties*; Kennedy, J. F., Phillips, G. O., Williams, P. A., Eds.; Ellis Horwood: New York 1990; pp 3−12.
(29) Kuga, S.; Brown, R. M., Jr. Lattice imaging of ramie cellulose. *Polym. Commun.* **1987**, *28*, 311−314.
(30) Roche, E.; Chanzy, H. Electron microscopy study of the transformation of cellulose I into cellulose III_I in *Valonia*. *Int. J. Biol. Macromol.* **1981**, *3*, 201−206.
(31) Chanzy, H.; Henrissat, B.; Vuong, R.; Revol, J. F. Structural changes of cellulose crystals during the reversible transformation cellulose I→III_I in *Valonia*. *Holzforschung* **1986**, *40* (Suppl.), 25−30.
(32) Sugiyama, J.; Harada, H.; Saiki, H. Crystalline morphology of *Valonia macrophysa* cellulose III_I revealed by direct lattice imaging. *Int. J. Biol. Macromol.* **1987**, *9*, 122−130.
(33) Chanzy, H.; Henrissat, B.; Vincendon, M.; Tanner, S. F.; Belton, P. S. Solid-state ^{13}C NMR and electron microscopy study on the reversible cellulose I−cellulose III_I transformation in *Valonia*. *Carbohydr. Res.* **1987**, *160*, 1−11.
(34) Bradford, H.; Revol, J. F. In *Cellulose and Wood. Chemistry and Technology*; Schuerch, C., Ed.; Wiley-Interscience: New York, 1989; pp 129−138.
(35) Okano, T.; Sarko, A. Mercerization of cellulose. II. Alkali-cellulose intermediates and a possible mercerization mechanism. *J. Appl. Polym. Sci.* **1985**, *30*, 325−332.
(36) Maurer, A.; Fengel, D. Parallel orientation of the molecular chains in cellulose I and cellulose II deriving from higher plants. *Holz Roh−Werst.* **1992**, *50*, 493.
(37) Dinand, E.; Vignon, M.; Chanzy, H.; Heux, L. Mercerization of primary wall cellulose and its implication for the conversion of cellulose I→cellulose II. *Cellulose* **2002**, *9*, 7−18.
(38) Shibazaki, H.; Kuga, S.; Okano, T. Mercerization and acid hydrolysis of bacterial cellulose. *Cellulose* **1997**, *4*, 75−87.
(39) Chanzy, H.; Roche, E. J. Fibrous mercerization of *Valonia* cellulose. *J. Polym. Sci., Polym. Phys. Ed.* **1975**, *13*, 1859−1862.
(40) Purz, H. J.; Fink, H. P. Morphology and lattice transition during alkaline treatment of cellulose. *Acta Polym.* **1983**, *34*, 546−558.

BM0506391